Scientific Research Publishing

Journal of Applied Mathematics and Physics, 2022, 10, 1325-1334
https://www.scirp.org/journal/jamp
ISSN Online: 2327-4379
ISSN Print: 2327-4352

Accelerating the Feedback Loop in Scanning Probe Microscopes without Loss of Height Measurement Accuracy by Using Pixel Forecast Methods

Robert Köhn, Boris Braun, Kai-Felix Braun

Engineering Department, Wilhelm Büchner University of Applied Sciences, Darmstadt, Germany
Email: kai_braun@gmx.de

How to cite this paper: Köhn, R., Braun, B. and Braun, K.-F. (2022) Accelerating the Feedback Loop in Scanning Probe Microscopes without Loss of Height Measurement Accuracy by Using Pixel Forecast Methods. *Journal of Applied Mathematics and Physics*, **10**, 1325-1334.
https://doi.org/10.4236/jamp.2022.104093

Received: March 9, 2022
Accepted: April 25, 2022
Published: April 28, 2022

Abstract

Scanning probe microscopes (SPM) are limited in their speed of data acquisition by the mechanical stability of the scanner. Therefore many types of scanners have been developed to achieve a rigid setup while maintaining an acceptable image size. We have followed here a different path to accelerate data acquisition by improving the feedback loop to achieve the same SPM image quality in a shorter time. While the feedback loop in a scanning probe microscope typically starts to probe a new pixel starting from the previous position, we have reduced the total control time by using an improved starting point for the feedback loop at each pixel. By exploiting the information of the already scanned pixels a forecast for the new pixel is created. We have successfully used several simple methods for a prognosis in MATLAB simulations like one dimensional linear or cubic extrapolation and others. Only scanning tunnelling microscope data from real experiments were used to test the forecasts. A doubling of the speed was achieved in the most favourable cases.

Keywords

Scanning Probe Microscopy, Feedback Loop, Controller Simulation

1. Introduction

Scanning probe microscopy (SPM) is a well-established and extremely powerful technique for the structural analysis of surfaces and thin films. Thereby scanning tunnelling microscopy (STM), atomic force microscopy (AFM), scanning near

field microscopy (SNOM) and more, have all in common that a local probe is used to determine a surface property. Thereby typically this signal is height dependent and the height is regulated with a feed-back loop to determine the height of the set point value. After regulation the new height is saved as a new pixel which is then used as the starting point for the regulation of the next pixel. We show in this article that an improved starting point can accelerate the speed of the data acquisition. The improvement is a forecast of the next pixel on the basis of the prior pixels so that a reduced height difference has to be overcome by the feed-back loop.

Some work has been published recently dealing with the simulation of the feedback loop of SPM [1]-[7]. In this article we have used simulations of the feed-back loop of a specific STM [8] [9] but regardless of the specific properties the results of the investigations are valid in general and apply to all SPM.

The fundamental assumption the here presented procedure is based on, is that the settling time to achieve a vanishing stead-state error increases with step height. To prove this assumption we have simulated the feedback loop and determined the settling time versus the applied step height. **Figure 1** shows the result for two different types of feedback loops, a proportional and integral control (PI) with the following difference equation [10]:

$$u(k) = u(k-1) + a \cdot e(k) + a_2 \cdot e(k-1) \tag{1}$$

and a proportional and first order delay control (PT1) with the following difference equation [11]:

$$u(k) = c \cdot e(k) + c_2 \cdot u(k-1) \tag{2}$$

The coefficients c_1 and c_2 were chosen from real data [9] and the formulas (1) respectively (2) were embedded in an STM simulation as described below. Thereby

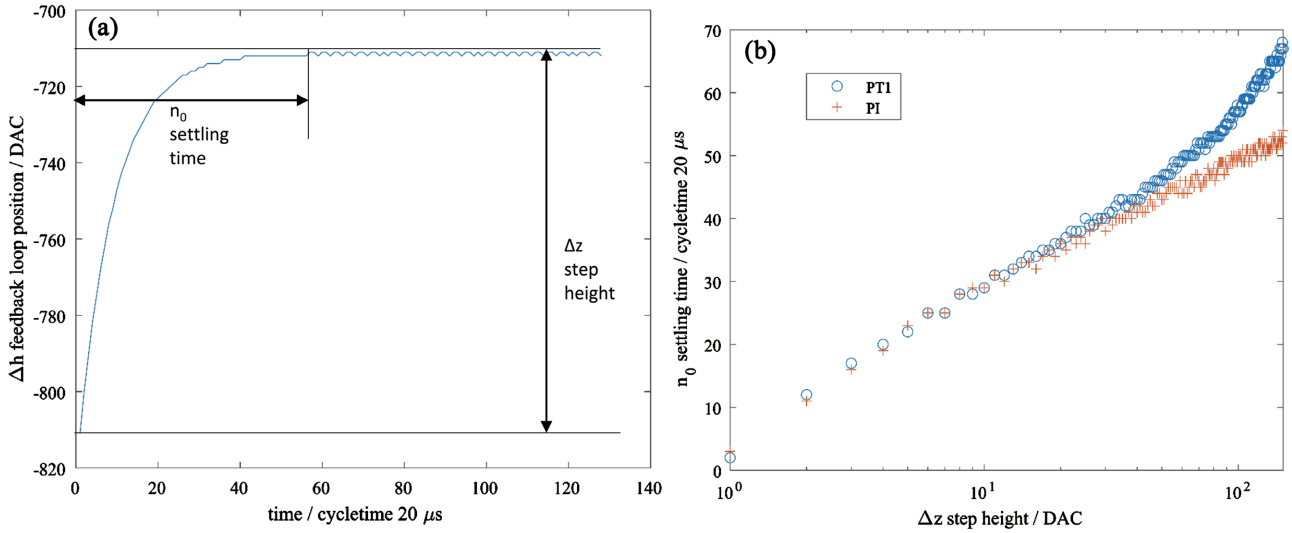

Figure 1. (a) Step response of a PT1 feedback loop. (b) Settling time n_0 versus step height Δz. The values have been determined using simulations with a PT1 and a PI feedback loop. Independent of the feedback loop type there is a logarithmic increase of the settling time versus the step height.

a step function with height Δz was fed into the simulation and the settling time n_0 was determined when the tip height difference Δh becomes equal to Δz. The progression of the tip height is depicted in **Figure 1(a)** for a PT1 controller. Variation of the step height resulted then in the graph in **Figure 1(b)**. The coefficients a1 and a2 for the PI controller were then adjusted to yield the same settling time for $\Delta z = 10$ DAC as the PT1 controller to ensure the same speed of the feed-back loop. By doing so, a direct comparison of the two controller types with respect to the settling time becomes possible.

Both controllers show an almost logarithmic increase of the settling time over a wide range of step heights. We conclude, that the settling time increases with step height for both controller types. Therefore a successful pixel forecast should reduce the effective step height and thereby the settling time. By doing so the overall time required for data acquisition is reduced which will be shown in the next section.

2. Materials and Methods

The here simulated STM data acquisition system has a digital control at an analogue control section. The feedback loop is constituted by the high voltage amplifier, the z-piezo actuator, the tunnelling junction, the I-V-converter, the analogue to digital converter and the digital signal processor card [10] [11]. Latter one was a PC32 DSP from Innovative Integration with a cycle rate of 50 kHz. To mimic this system the following formulas were implemented in MATLAB displaying the feedback loop. SIMULINK may have been used as well but was not because implementing the feedback loop was eased by using MATLAB only. The consecutive formulas were repeated times the number of cycles per pixel:

$$\left.\begin{aligned}
i_{tunneling} &= i_{target} \cdot \mathrm{e}^{2\cdot\kappa\cdot(\Delta z+\Delta h)} \\
adc_{value} &= \left\lceil i_{tunneling} \cdot gain_{IV} \cdot \frac{2^{16}}{20} \right\rceil \\
diff &= \log_{10}\left(adc_{value} \cdot \frac{10000}{32767} \right) - fconi_{log} \\
u(k) &= c_1 \cdot diff + c_2 \cdot u(k-1) \\
dac_{value} &= \lceil u(k) \rceil \\
piezo_{voltage} &= dac_{value} \cdot \frac{20}{2^{16}} \cdot gain_z \\
\Delta h &= piezo_{voltage} \cdot z_{const}
\end{aligned}\right\} \quad (3)$$

Hereby $fconi_{log}$ is the $\log_{10}$ value of the set point current and *diff* the deviation from it. The parameter c_1 and c_2 determine the PT1 controller. Δz is the step height in nm to be overcome and Δh is the height change in nm, please refer also to **Figure 1(a)** for their definitions. The dac_{value} is the current tip position in DAC units. The course of the controller is saved in the array *u(k)*. The exponential for the calculation of the current in the first line does not carry a minus sign

as expected from literature since here $\Delta z + \Delta h$ denote the displacement of the tunnelling tip and not the distance from the surface. The ADC and DAC had a 16 bit resolution on ±10 V voltage.

Real data from low temperature scanning tunnelling microscopy experiments was used as test data [9]. Thereby care was taken that surfaces with different corrugations were chosen. Some of the data is shown in the next section of this article. The parameter c_1, c_2, $gain_{IV}$ and $fconi_{log}$ had been set in the experiments and are part of the test data. κ is an experimentally determined constant [9].

So the image was scanned in the simulation pixel by pixel and line by line using the Δz in nm of each pixel as input for the above displayed feedback loop. This Δz is adjusted for a better starting value by the use of a forecast $\Delta_{\Delta z}$. Thereby a linear one dimensional (1d),

$$\Delta_{\Delta z} = m \cdot x + b \tag{4}$$

a cubic one dimensional,

$$\Delta_{\Delta z} = \alpha \cdot x^3 + \beta \cdot x^2 + \gamma \cdot x + \delta \tag{5}$$

and the two-dimensional *gridfit* MATLAB method and more were used. The coefficients in (5) and (7) were obtained by a least chi-square-fit. The *gridfit* MATLAB method uses one of either three methods: Interpolation of the next neighbour, triangular interpolation or bilinear interpolation. It is particularly well suited for the forecast of pixel at the brim of an area.

The forecast requires a certain number of pixels as historical data within the same line or around the pixel, therefore no forecast was used in the first two columns of the image for the linear prediction, and no forecast was used in the first four columns for the cubic prediction and so on.

3. Results

Figure 2(a) displays an image recorded with a scanning tunnelling microscope at 4 K. Segmented flat areas of the Ag (111) surface are visible, separated by single atomic steps. **Figure 2(b)** shows a horizontal linescan revealing rather smooth transitions between the pixels. This image has been taken as input for the above described simulations.

First, the original feedback loop was used to simulate the scan of the image at the original speed of 64 cycles per pixel. Then the resulting image was subtracted from the experimental data and the absolute deviation summed over the whole image. This value was then used as a metric for the image quality. **Figure 3** shows the metric values for different forecasting methods and scanning speeds e.g. number of cycles per pixel.

The original method without forecast should show actually a value of zero at the original experimentally used number of cycles per pixel of 64 because 64 was used in the experiment, but it does not. We attribute the deviation to the shortcomings of our implemented model and the round off errors in the numerical simulations. The implemented model of the STM does not include the impedances of cables and the actuator piezos and the mechanical properties of these.

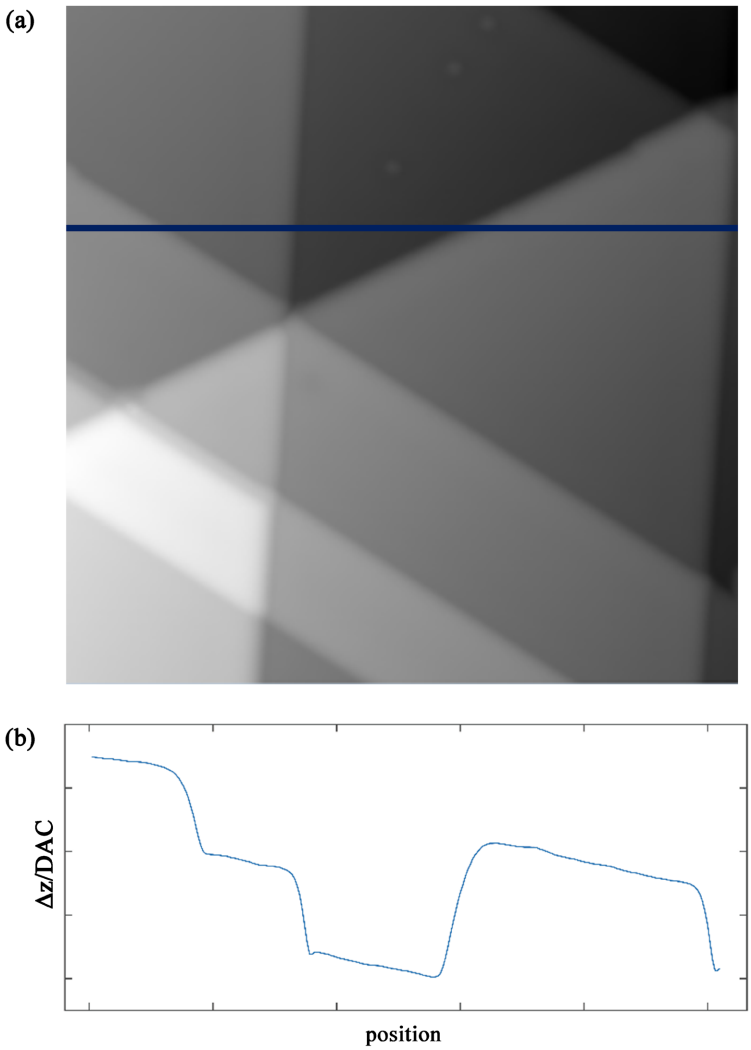

Figure 2. (a) A 37.5 nm × 37.5 nm STM image of the Ag (111) surface at 4 K nearby a tip indention into the surface. (b) A horizontal linescan showing rather smooth transitions between the pixels. (a) A 37.5 nm × 37.5 nm STM image of the Ag (111) surface at 4 K nearby a tip indention into the surface. (b) A horizontal linescan showing rather smooth transitions between the pixels.

Furthermore the rounding algorithm of the DACs and ADCs of the signal processor card is not known either and had to be therefore assumed. Last but not least a number of intermediate regulation steps were taken in the original STM instead of a single large step. These are the reasons for a minor numerical instability to occur in the simulations which is visible in **Figure 1(a)** at the end of the graph. There the values of the feedback loop oscillate by one DAC unit instead of being completely stable. As a result the metric for the whole image is not zero, even with experimentally used number of cycles per pixel. On the other hand show the simulations with forecast sometimes zero error. There the forecast resulted in a compensation of the above mentioned error sources.

Figure 3 shows as well results from scans with smaller number of cycles per pixel e.g. higher speed. The deviation metric shows a pronounced rise as the

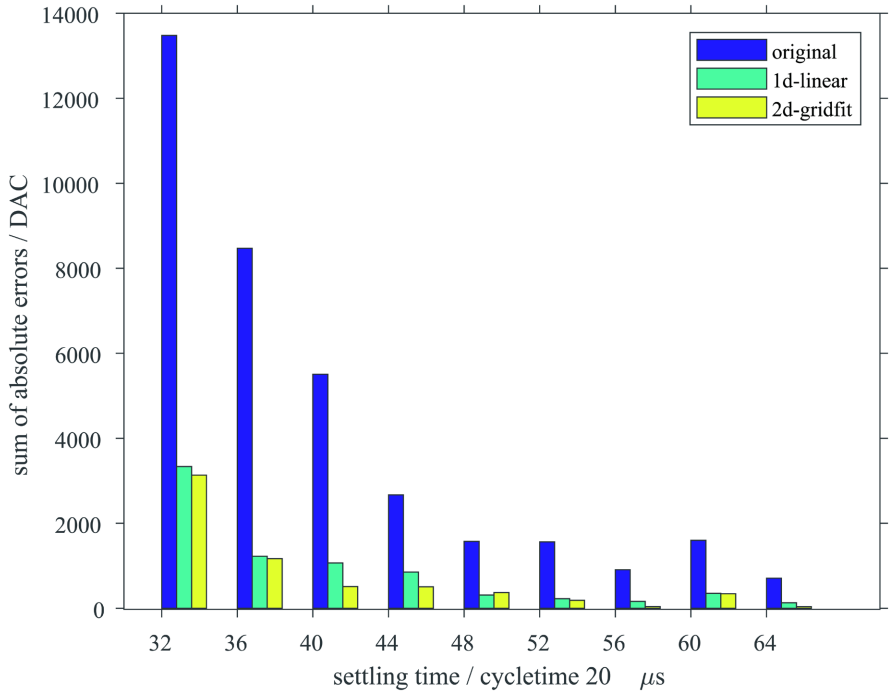

Figure 3. Simulation results for the image in **Figure 2(a)** displaying the deviation of an image scan with pixel forecast from an ideal image scan taken with 64 cycles per pixel without pixel forecast. The erroneous deviation increases with decreasing number of cycles per pixel. The two alternative methods with pixel forecast clearly show improved results over the original feedback loop without forecasting.

number of cycles is decreased. At small numbers of cycles the time is not sufficient anymore for the feedback loop to complete the regulation. This situation is improved by using pixel forecast methods for the respective next pixel. **Figure 3** shows results with a one dimensional linear forecast and with a two dimensional forecast which is using the gridfit MATLAB method. The latter yielded similar results as the 1d-linear forecast although it exploits the two dimensional area surrounding the respective next pixel.

The values for the deviation metric at 35 cycles per pixel do not substantially differ from the values at 64 cycles, the original number. In fact, even the simulated image at 32 cycles is optically not distinguishable from the original one with 64 cycles. We therefore conclude that the speed of data acquisition can indeed be doubled without loss of image quality.

Figure 4 shows a rather different topography. Here an artificial atomic structure at 4 K is displayed. Again the transitions between the pixels are rather smooth and the profile is steady. These are good conditions for a forecast and actually the forecast methods show again good performance as depicted in **Figure 5**. There in some cases were even no errors using a forecast, showing the improved quality by the forecast methods. More methods have been tested, including cubic extrapolation, averaging methods and combination of these. The outcome of these simulations are not shown here, but are mixed and yield similar results as compared to those in **Figure 3** and **Figure 5** [11].

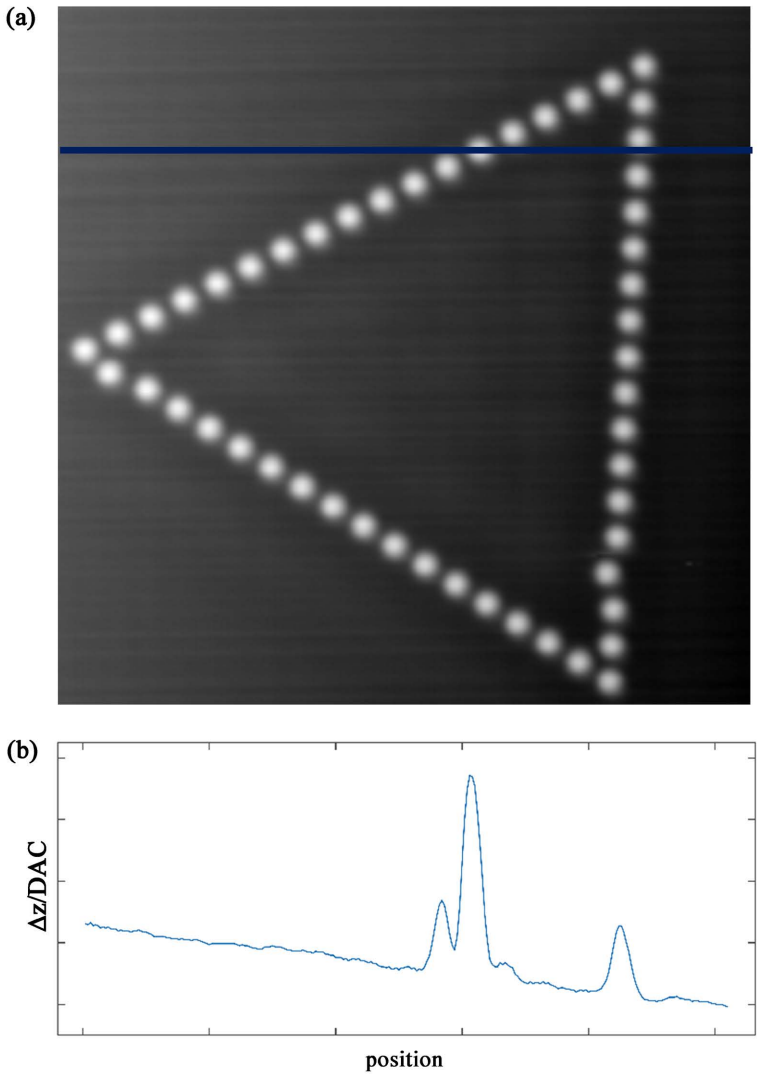

Figure 4. (a) A 28.1 nm × 28.1 nm stm image of the Ag (111) surface at 4 K showing an artificial atomic structure from 51 Ag atoms. (b) A horizontal linescan showing again rather smooth transitions between the pixels.

More topographies have been tested, a selection can be seen in **Figure 6**. In **Figure 6(a)** the Ag (111) surface has been atomically resolved. The corresponding horizontal linescan can be seen in **Figure 6(b)** and shows a signal at the resolution limit of the ADC. Although the single atoms are clearly visible in the image, the signal counts only 1 - 3 DAC units. Even more, the noise level appears to be of similar strength, as is apparent from the image data. Therefore it is not surprising that the forecasting methods fail for this image.

In **Figure 6(c)** the Cr (110) surface has been resolved. Several flat terraces can be seen, separated by atomic steps. On the terraces, adsorbates are displayed as dark indentions. The horizontal linescan in **Figure 6(d)** shows the high number of adsorbates as dips in the curve. Again the forecast methods yield no advantage for this image. We conclude that high frequency modulations like the kind in **Figure 6(c)** are not suited for linear or cubic forecast methods.

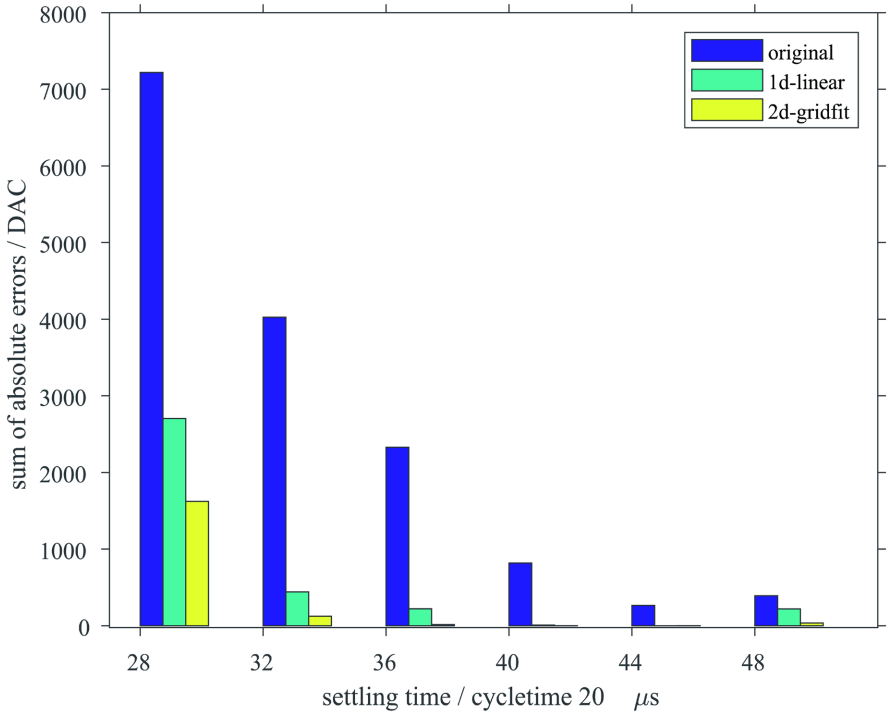

Figure 5. Simulation results for the image in **Figure 4(a)** displaying the deviation of an image scan with pixel forecast from an ideal image scan taken with 48 cycles per pixel without pixel forecast. Again the two alternative methods with pixel forecast clearly show improved results over the original feedback loop without forecasting.

4. Discussion

To summarize, we have presented a method to increase the speed of data acquisition in SPM. The increasingly computational more powerful signal processor cards make it possible to use intelligent and complex regulators. Therefore such forecast methods can easily be implemented. We were able to prove that linear forecasts improve the acquisition speed substantially and can even double it. We showed also the limitations of this method which are given by poor signal-to-noise data or high frequency modulation of the data.

Although the approach presented in this article may resemble of a feedforward control approach as discussed in [12], it differs by not altering the speed of the feed-back loop itself but instead reducing the time which is spent on each pixel. In that sense the electromechanical dynamics of the scanner and the feed-back loop are not altered.

A moving-average-time series (MA) approach has been investigated by one of the co-authors in [13]. It showed good results for tilted surfaces but not as good as the results shown here. An inclination between the tip measurement plane and the surface plane is usually present and can thus be compensated but does not consider local details. Future work can be done using auto-regressive-time series (AR) approach or even ARMA or ARMA-GARCH. A simpler method from financial forecasting would be to use a Kalman-filter, a linear predictor for noise

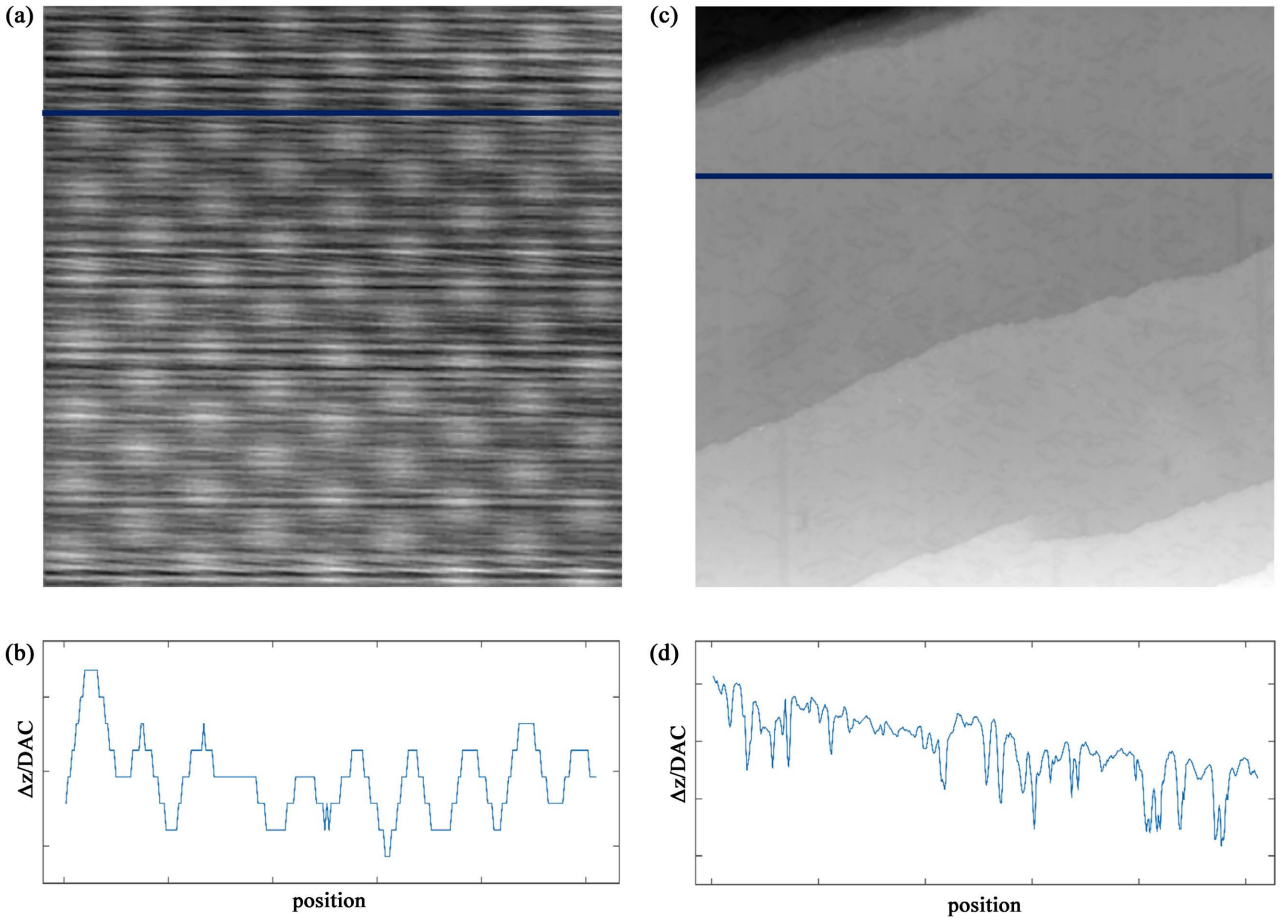

Figure 6. (a) A 2.34 nm × 2.34 nm STM image of the Ag (111) surface at 4 K showing atomic resolution. (b) A horizontal linescan from (a) showing the poor vertical resolution. (c) A 124 nm × 124 nm stm image of the Cr (110) surface at 77 K showing several atomic steps and adsorbates on them. (d) A horizontal linescan from (c) showing high frequency modulation.

affected data.

At this point we point out, that we have used feedback gains which were obtained experimentally. These feedback gains cannot be increased further, otherwise the mechanical resonances of the piezo system would be triggered, resulting in artefacts in the images. These mechanical resonances are not included in the used model, putting therefore a limitation to the realistic description of the used setup. Because of that and because only the recorded forward image pixels were used, we consider this study rather as a proof of concept. Future work might include implementation in an experimental setup and the robustness analysis of this approach to the quantization, the fitting dilemma.

5. Conclusion

The here presented method can be applied not only to STM but to all SPM methods in general to accelerate data acquisition.

Conflicts of Interest

The authors declare no conflicts of interest regarding the publication of this paper.

References

[1] Stirling, J. (2014) Control Theory for Scanning Probe Microscopy Revisited. *Beilstein Journal of Nanotechnology*, **5**, 337-345. https://doi.org/10.3762/bjnano.5.38

[2] Hagmann, M.J., Spencer, G. and Wiedemeier, J. (2018) Virtual Scanning Tunnelling Microscope Offered as a Free-Download. *Micros Today*, **26**, 18-23. https://doi.org/10.1017/S1551929518000019

[3] Wiedemeier, J., Spencer, G., Hagmann, M.J. and Mousa, M.S. (2019) Simulation and Analysis of Methods for Scanning Tunneling Microscopy Feedback Control. *Microscopy and Microanalysis*, **25**, 1-7. https://doi.org/10.1017/S1431927619000278

[4] Huang, W.W., Guo, P., Hu, C. and Zhu, L.M. (2022) High-Performance Control of Fast Tool Servos with Robust Disturbance Observer and Modified H∞ Control. *Mechatronics*, **84**, Article ID: 102781. https://doi.org/10.1016/j.mechatronics.2022.102781

[5] Huang, W.W., Li, L., Li, Z.L., Zhu, Z. and Zhu, L.M. (2021) Robust High-Bandwidth Control of Nano-Positioning Stages with Kalman Filter Based Extended State Observer and H∞ Control. *Review of Scientific Instruments*, **92**, Article ID: 065003. https://doi.org/10.1063/5.0048870

[6] Yang, R., Wang, M., Li, L., Wang, G. and Zhong, C. (2019) Robust Predictive Current Control of PMLSM with Extended State Modeling Based Kalman Filter: For Time-Varying Disturbance Rejection. *IEEE Transactions on Power Electronics*, **35**, 2208-2221. https://doi.org/10.1109/TPEL.2019.2923631

[7] Habibullah, H., Pota, H.R. and Petersen, I.R. (2014) High-Speed Spiral Imaging Technique for an Atomic Force Microscope Using a Linear Quadratic Gaussian Controller. *Review of Scientific Instruments*, **85**, Article ID: 033706. https://doi.org/10.1063/1.4868249

[8] Binning, G., Rohrer, H., Gerber, G. and Weibel, E. (1982) Tunneling through a Controllable Vacuum Gap. *Applied Physics Letters*, **40**, 178-180. https://doi.org/10.1063/1.92999

[9] Braun, K.-F. (2001) Investigation of Surfaces and Atomic Manipulation with a Scanning Tunnelling Microscope at Low Temperature. PhD Thesis, Freie Universität, Berlin, Germany.

[10] Poley, R. (2015) Control Theory Fundamentals. 3rd Edition, CreateSpace.

[11] Köhn, R. (2020) Performanceoptimierung der Regelung für ein Rastertunnelmikroskop durch Prognoseverfahren. Bachelor Thesis, Wilhelm Büchner University of Applied Sciences, Darmstadt, Germany.

[12] Clayton, G.M., Tien, S., Leang, K.K., Zou, Q. and Devasia, S. (2009) A Review of Feedforward Control Approaches in Nanopositioning for High-Speed SPM. *Journal of Dynamic Systems, Measurement, and Control*, **131**, Article ID: 061101. https://doi.org/10.1115/1.4000158

[13] Braun, B. (2019) Geschwindigkeitsoptimierung einer Höhenregelung für Rastersondenverfahren mittels Vorregelung anhand von Prognosedaten. Bachelor Thesis, Wilhelm Büchner University of Applied Sciences, Darmstadt, Germany.